

## STABILITY OF ACCRETION DISKS AROUND ROTATING BLACK HOLES: A PSEUDO-GENERAL-RELATIVISTIC FLUID DYNAMICAL STUDY

BANIBRATA MUKHOPADHYAY

Inter-University Centre for Astronomy and Astrophysics, Post Bag 4, Ganeshkhind, Pune 411 007, India

Received 2002 September 8; accepted 2002 December 6

### ABSTRACT

We discuss the solution of an accretion disk when the black hole is chosen to be rotating. We study how the fluid properties are affected for different rotation parameters of the black hole. We know that no cosmic object is static in the universe. Here the effect of the rotation of the black hole on spacetime is considered, following an earlier work of the author, where the pseudo-Newtonian potential was prescribed for the Kerr geometry. We show that, with the inclusion of rotation of the black hole, the valid disk parameter region dramatically changes, and the disk becomes unstable. Also we discuss the possibility of shocks in accretion disks around rotating black holes. When the black hole is chosen to be rotating, the sonic locations of the accretion disk get shifted or disappear, making the disk unstable. To bring it into the stable situation, the angular momentum of the accreting matter has to be reduced/enhanced (for co/counterrotating disk) by means of some physical process.

*Subject headings:* accretion, accretion disks — black hole physics — gravitation — hydrodynamics — shock waves

### 1. INTRODUCTION

Over the last three decades, fluid dynamical studies of accretion disks around black holes have been extensively performed. Shakura & Sunyaev (1973) initiated this discussion considering a very simplistic but effective model of accretion disks. They chose the Newtonian gravitational potential. Novikov & Thorne (1973) and Page & Thorne (1974) studied a few aspects of the accretion disk in a fully relativistic treatment. Paczyński & Wiita (1980) proposed one pseudopotential which could approximately describe relativistic properties of the accretion disk around nonrotating black holes. Using that pseudopotential, Abramowicz & Zurek (1981) studied some transonic properties of accretion flows. With time, a number of studies of accretion disks have been carried out with modified disk structures (e.g., Abramowicz et al. 1988; Abramowicz & Kato 1989; Chakrabarti 1990, 1996a; Narayan & Yi 1994; Narayan et al. 1997, 1998; Kato, Fukue, & Mineshige 1998; Mukhopadhyay 2002a) for nonrotating black holes. Also the studies of accretion disks in Kerr geometry have been explored by several authors (e.g., Sponholz & Molteni 1994; Chakrabarti 1996b, 1996c; Abramowicz et al. 1996; Peitz & Appl 1997; Gammie & Popham 1998; Popham & Gammie 1998; Miwa et al. 1998; Lu & Yuan 1998; Manmoto 2000). Those studies have been made either in a full general relativistic or in a pseudo-Newtonian approach.

The study of stability of the accretion disk is one of the important criteria in this context. The possibility of steady and stable disk formation by incoming matter toward a black hole is allowed only for certain sets of initial parameters. Abramowicz & Zurek (1981) studied the effect of angular momentum on the accretion and the corresponding stability of the transonic nature of the infalling matter onto the black hole. After that, Chakrabarti (1989, 1990) discussed the formation of sonic points and shock waves in accretion disks. He showed that the formation of stable sonic points and shocks in the disk are possible for a particular range of physical parameters. Recently, Mukhopad-

hyay & Chakrabarti (2001) have analyzed the stability of accretion disk in the presence of nucleosynthesis. As the temperature of the disk is very high (at least of the order of  $10^9$  K), nuclear burning can take place and generate and/or absorb energy on a large scale in the disk. Because of this generation/absorption of nuclear energy, fundamental properties of the disk, like sonic locations, temperature, Mach number, shock location (if any), etc., may be affected. Thus the stability gets influenced by the nuclear burning. If the rate of generation/absorption of nuclear energy is large, the disk structure may become unstable. In their discussion, Mukhopadhyay & Chakrabarti (2001) have also shown that the sonic locations disappear for a particular shell of an accretion disk where the nuclear energy is significant compared to the mechanical energy of the accreting matter.

In all the above mentioned works, when the stability was analyzed for the accretion disk, the central black hole was chosen to be nonrotating. As it is well known that no object is static in the universe, before making any serious conclusions about the inner properties of the accretion disk, consideration of rotation of a black hole is essential. Though a few works have been done for Kerr black holes, no such comparative study has been explored so far with different Kerr parameters. Thus, automatically, two questions arise. Does the rotation of the black hole play an important role in the accretion properties of a disk? Does the consideration of rotation of the black hole affect the disk structure for a particular parameter regime that is known to be stable for the nonrotating case? Here, we would like to address these questions one by one.

Recently, we have proposed a new pseudo-Newtonian potential (Mukhopadhyay 2002b, hereafter Paper I) to describe the accretion disk around Kerr black holes. Following Paper I, we will describe our accretion disk in a pseudo-Newtonian manner. The potential that we are using can describe approximately all the essential general relativistic properties of the accretion disk. It can reproduce the locations of marginally stable and bound orbits exactly or almost exactly for different Kerr parameters (see Paper I),

which are the pure general relativistic properties. Therefore, we call this study a *pseudo-general-relativistic approach*. As our main interest is to study the inner region of the accretion disk, we will concentrate upon the sub-Keplerian flow, where the effect of rotation of the black hole is significant. In Paper I, we already raised several questions, which are important to address in the physics of accretion disk. Here we will show how useful the pseudopotential described in Paper I is in studying the global behavior of the accretion disk. In full general relativity, the basic equations of the accretion disk are very complicated and tedious to handle. In early works, there were no suitably good pseudopotentials for a rotating black hole. It seems that Paper I has come up with the answer, and one of our aims in this paper is to show its applicability. As the location of horizon, marginally bound and marginally stable orbits change for different Kerr parameters, any inner property of the disk is very much related to the rotation of black hole. We will follow Mukhopadhyay & Chakrabarti (2001) to analyze the stability of the disk. We will study whether or not the sonic location(s), shock formation(s) (if any), etc., get affected by applying rotation to the black hole. In an accretion disk, if the sonic point loses entropy or disappears by the rotational effect of black hole, we will understand that the sonic point as well as the disk is unstable because a stable sonic point is necessary for accretion onto the black hole. In the next section, we will present the basic equations needed to describe the accretion disk. In § 3, we will discuss about the parameter space of accretion disk and how the rotation affects it. Subsequently, in § 4, we will describe the fluid dynamical results. Finally, in § 5, we will sum up all the results and make the overall conclusions.

## 2. BASIC EQUATIONS

Throughout in our calculations, we express the radial coordinate in units of  $GM/c^2$ , where  $M$  is the mass of the black hole,  $G$  is the gravitational constant, and  $c$  is the speed of light. We also express the velocity in units of the speed of light and the angular momentum in units of  $GM/c$ . The equations to be solved are given below as

$$\frac{d}{dx}(x\Sigma v) = 0, \quad (1)$$

$$v \frac{dv}{dx} + \frac{1}{\rho} \frac{dP}{dx} - \frac{\lambda^2}{x^3} + F(x) = 0, \quad (2)$$

where  $\Sigma$  is the vertically integrated density and  $F(x)$  is the gravitational pseudo-Newtonian force given in Paper I as

$$F(x) = \frac{(x^2 - 2a\sqrt{x} + a^2)^2}{x^3[\sqrt{x}(x-2) + a]^2}, \quad (3)$$

where  $a$  indicates the specific angular momentum of the black hole (the Kerr parameter). We do not consider any kind of energy dissipation in the accretion disk, as we want to check how the black hole rotation solely can affect the disk properties. Thus the angular momentum of the accreting fluid ( $\lambda$ ) remains constant throughout a particular flow. Following Matsumoto et al. (1984), we can calculate the vertically integrated density as

$$\Sigma = I_n \rho_e h(x), \quad (4)$$

where  $\rho_e$  is the density at equatorial plane,  $h(x)$  is the half-thickness of the disk, and  $I_n = (2^n n!)^2 / [(2n+1)!]$ , where  $n$  is the polytropic index. From the vertical equilibrium assumption, the half-thickness can be written as

$$h(x) = c_s x^{1/2} F^{-1/2}, \quad (5)$$

where  $c_s$  is the speed of sound. We also consider the equation of state to be  $\gamma P / \rho = c_s^2$ , where  $\gamma$  is the gas constant.

Now, combining equations (1) and (2) we get

$$\frac{dv}{dx} = \left[ \frac{\lambda^2}{x^3} - F(x) + \frac{c_s^2}{\gamma+1} \left( \frac{3}{x} - \frac{1}{F} \frac{dF}{dx} \right) \right] / \left[ v - \frac{2c_s^2}{(\gamma+1)v} \right]. \quad (6)$$

Far away from the black hole,  $v < c_s$ , and close to it,  $v > c_s$ , thus there is an intermediate location where the denominator of equation (6) must vanish. Therefore, to have a smooth solution at that location, the numerator has to be zero. This location is called the sonic point or critical point ( $x_c$ ). The existence of this sonic location plays an important role in the accretion phenomena. For an accretion disk around a black hole, a sonic point must exist. From the global analysis of a sonic point, one can understand the stability of the physical parameter region that we will discuss in the next section.

As it is described above that at  $x = x_c$ ,  $dv/dx = 0/0$ , using l'Hôpital's rule and after some algebra, we can get the velocity gradient of accreting matter at the sonic location as

$$\left. \frac{dv}{dx} \right|_c = - \frac{\mathcal{B} + \sqrt{\mathcal{B}^2 - 4\mathcal{A}\mathcal{C}}}{2\mathcal{A}}, \quad (7)$$

where

$$\begin{aligned} \mathcal{A} &= 1 + \frac{2c_{sc}^2}{(\gamma+1)v_c^2} + \frac{4c_{sc}^2(\gamma-1)}{v_c^2(\gamma+1)^2}, \\ \mathcal{B} &= \frac{4c_{sc}^2(\gamma-1)}{v_c(\gamma+1)^2} \left( \frac{3}{x_c} - \frac{1}{F_c} \frac{dF}{dx} \Big|_c \right), \\ \mathcal{C} &= \frac{c_{sc}^2}{\gamma+1} \left[ \left( \frac{1}{F_c} \frac{dF}{dx} \Big|_c \right)^2 - \frac{1}{F_c} \frac{d^2F}{dx^2} \Big|_c - \frac{3}{x_c^2} \right] - \frac{3\lambda^2}{x_c^4} - \frac{dF}{dx} \Big|_c \\ &\quad - \frac{c_{sc}^2(\gamma-1)}{(\gamma+1)^2} \left[ \frac{3}{x_c} - \frac{1}{F_c} \frac{dF}{dx} \Big|_c \right]^2. \end{aligned} \quad (8)$$

Thus, we have to integrate equations (6) and (7) with an appropriate boundary condition to get the fluid properties in the accretion disk. From equation (6), we can easily find out the Mach number at the sonic point as

$$M_c = \frac{v_c}{c_{sc}} = \sqrt{\frac{2}{\gamma+1}} \quad (9)$$

and the corresponding sound speed as

$$c_{sc} = \sqrt{(\gamma+1) \left( \frac{\lambda^2}{x_c^3} - F_c \right) \left( \frac{1}{F_c} \frac{dF}{dx} \Big|_c - \frac{3}{x_c} \right)^{-1}}. \quad (10)$$

Now integrating equations (1) and (2), we can write down the energy and entropy of the flow at a sonic point as

$$E_c = \frac{2\gamma}{(\gamma-1)} \left[ \left( \frac{\lambda^2}{x_c^3} - F_c \right) / \left( \frac{1}{F_c} \frac{dF}{dx} \Big|_c - \frac{3}{x_c} \right) \right] + V_c + \frac{\lambda^2}{2x_c^2}, \quad (11)$$

and

$$\dot{\mathcal{M}}_c = (\gamma K)^n \dot{M} = x_c^{3/2} F_c^{-1/2} (\gamma + 1)^{q/2} \times \left[ \left( \frac{\lambda^2}{x_c^3} - F_c \right) / \left( \frac{1}{F_c} \frac{dF}{dx} \Big|_c - \frac{3}{x_c} \right) \right]^{\gamma/(\gamma-1)}, \quad (12)$$

where  $K$  is basically the entropy of the system,  $V_c = (\int F dx)|_c$  and  $q = (\gamma + 1)/[2(\gamma - 1)]$ . Actually,  $\mathcal{M}$  itself is not entropy but carries the information about it. For a nondissipative system,  $\mathcal{M}$  is conserved for a particular  $\dot{M}$ , unless the shock forms there. We have to supply the sonic energy  $E_c$  as the boundary condition for a particular flow. Then from equation (11), we can find out the sonic location  $x_c$ . Therefore, knowing  $x_c$ , one can easily find out the fluid velocity and sound speed at the sonic point from equations (9) and (10) for a particular accretion flow. These have to be supplied as further boundary conditions of the flow.

Another important issue is the formation of the shock in the discussion of the accretion disk. Here, whenever we mention the shock, will mean the Rankine-Hugoniot shock (Landau & Lifshitz 1987). If we generalize the conditions to form a shock in accretion disk given by Chakrabarti (1989) to the case of a rotating black hole, we get

$$\frac{1}{2} M_+^2 c_{s+}^2 + n c_{s+}^2 = \frac{1}{2} M_-^2 c_{s-}^2 + n c_{s-}^2, \quad (13)$$

$$\frac{c_{s+}^\nu}{\dot{M}_+} \left( \frac{2\gamma}{3\gamma-1} + \gamma M_+^2 \right) = \frac{c_{s-}^\nu}{\dot{M}_-} \left( \frac{2\gamma}{3\gamma-1} + \gamma M_-^2 \right), \quad (14)$$

$$\dot{M}_+ > \dot{M}_-, \quad (15)$$

where

$$\dot{M} = M c_s^{2(n+1)} \frac{x_s^{3/2}}{\sqrt{F(x_s)}}. \quad (16)$$

Here, the subscripts “-” and “+” indicate the quantities just before and after the shock, respectively, and  $x_s$  indicates the shock location.  $M$  denotes the Mach number of the matter and  $\nu = (3\gamma - 1)/(\gamma - 1)$ . From equations (13)–(16), it is very clear that except the entropy expression, all remain unchanged with respect to the case of a nonrotating black hole. Also from equations (14) and (16), we get the shock invariant quantity as

$$C = \frac{[2/M_+ + (3\gamma - 1)M_+]^2}{M_+^2(\gamma - 1) + 2} = \frac{[2/M_- + (3\gamma - 1)M_-]^2}{M_-^2(\gamma - 1) + 2}, \quad (17)$$

which remains unchanged with respect to the nonrotating case. If all the conditions (13)–(15) and (17) are simultaneously satisfied by the matter, the shock will form in an accretion disk.

### 3. ANALYSIS OF THE PARAMETER SPACE

One of our aims is to check how the rotation affects the disk parameter region known for a Schwarzschild black hole. Therefore, we have to analyze globally the accretion disk properties around rotating black holes. We also have to check, how does the rotation of the black hole affect the sonic location, structure as well as the stability of disk. In Figure 1a, we show the variation of disk entropy as a func-

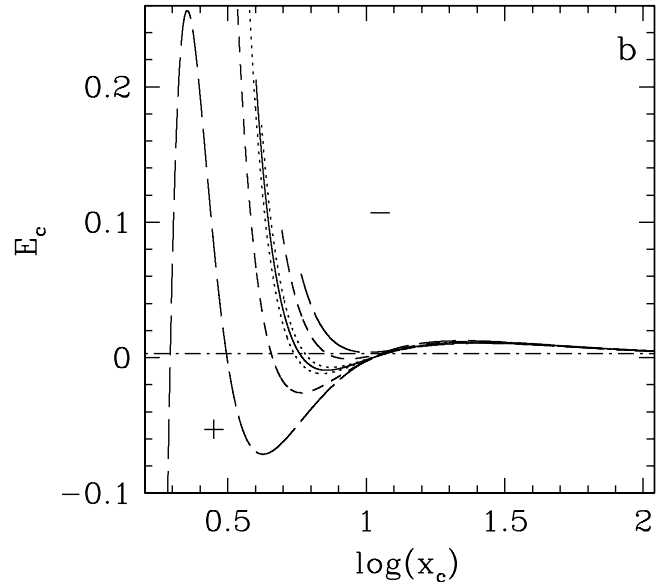
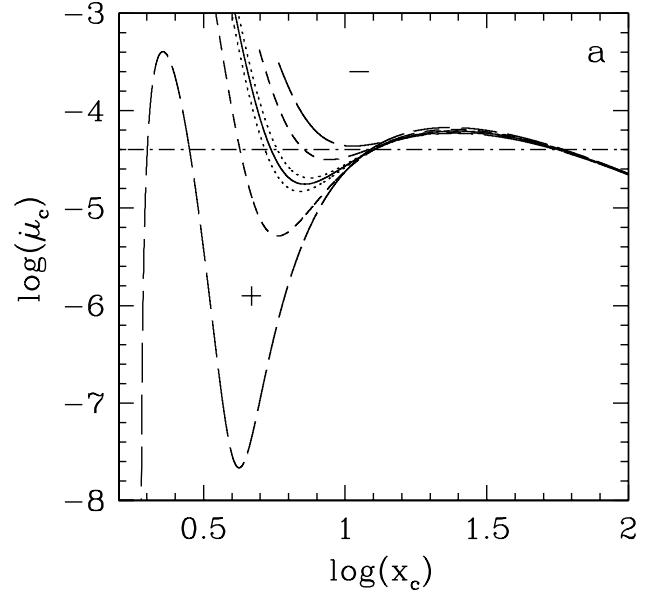


FIG. 1.—Variation of (a) entropy and (b) energy as a function of sonic location for various values of Kerr parameters  $a$ . Central solid line indicates nonrotating case ( $a = 0$ ), while the results in regions of either side of it indicated by “+” and “-” are for prograde and retrograde orbits, respectively. Different curves from the central solid line downward are for  $a = 0.1, 0.5, 0.998$  and upward for  $a = -0.1, -0.5, -0.998$ . The horizontal line indicates the curve of (a) constant entropy of  $5 \times 10^{-5}$  and (b) constant energy of 0.0065.  $\lambda = 3.3$ ,  $\gamma = 4/3$  for all the curves.

tion of sonic location. The intersections of all the curves by the horizontal line (which is a constant entropy line) indicate the sonic points of the accretion disk for that particular entropy and rotation of the black hole. It is clearly seen that, at a particular entropy, if the rotation of the black hole increases, marginally bound ( $x_b$ ) and stable ( $x_s$ ) orbits as well as sonic points shift to a more inner region and the possibility to have all four sonic points in the disk outside the horizon increases. As an example, for  $a = 0.998$ , the inner edge of the accretion disk enlarges in such a manner that the

fourth sonic point in the disk appears outside the horizon. On the other hand, for retrograde orbits (counterrotating cases),  $x_b$  and  $x_s$  move to greater radii, and all the sonic points come close together for a particular Kerr parameter. Similar features are reflected in Figure 1*b*, where the sonic energy is plotted as a function of sonic location. Here also, the intersections of the horizontal line (which indicates a constant energy line) with all the curves indicate the sonic points of the accretion disk for that particular energy and rotation of the black hole. For both Figures 1*a* and 1*b*, sonic points with negative slope of the curve indicate the locations of “saddle-type” sonic point and positive slopes indicate

the “center-type” sonic point. Thus the rotation of black hole plays an important role in the formation and location of sonic points which are related to the structure of accretion disk.

In Figure 2, with the consideration of rotation of black hole, we show how the disk region having three sonic points is affected. Figures 2*a*, 2*b*, and 2*c* show the variation of sonic entropy as a function of sonic point, when the angular momentum of accreting matter is chosen as the parameter for three different rotations of the black hole as  $a = 0.5, -0.5, 0$ . If we join the extrema of the curves, we get the bounded parameter region of the disk where the three

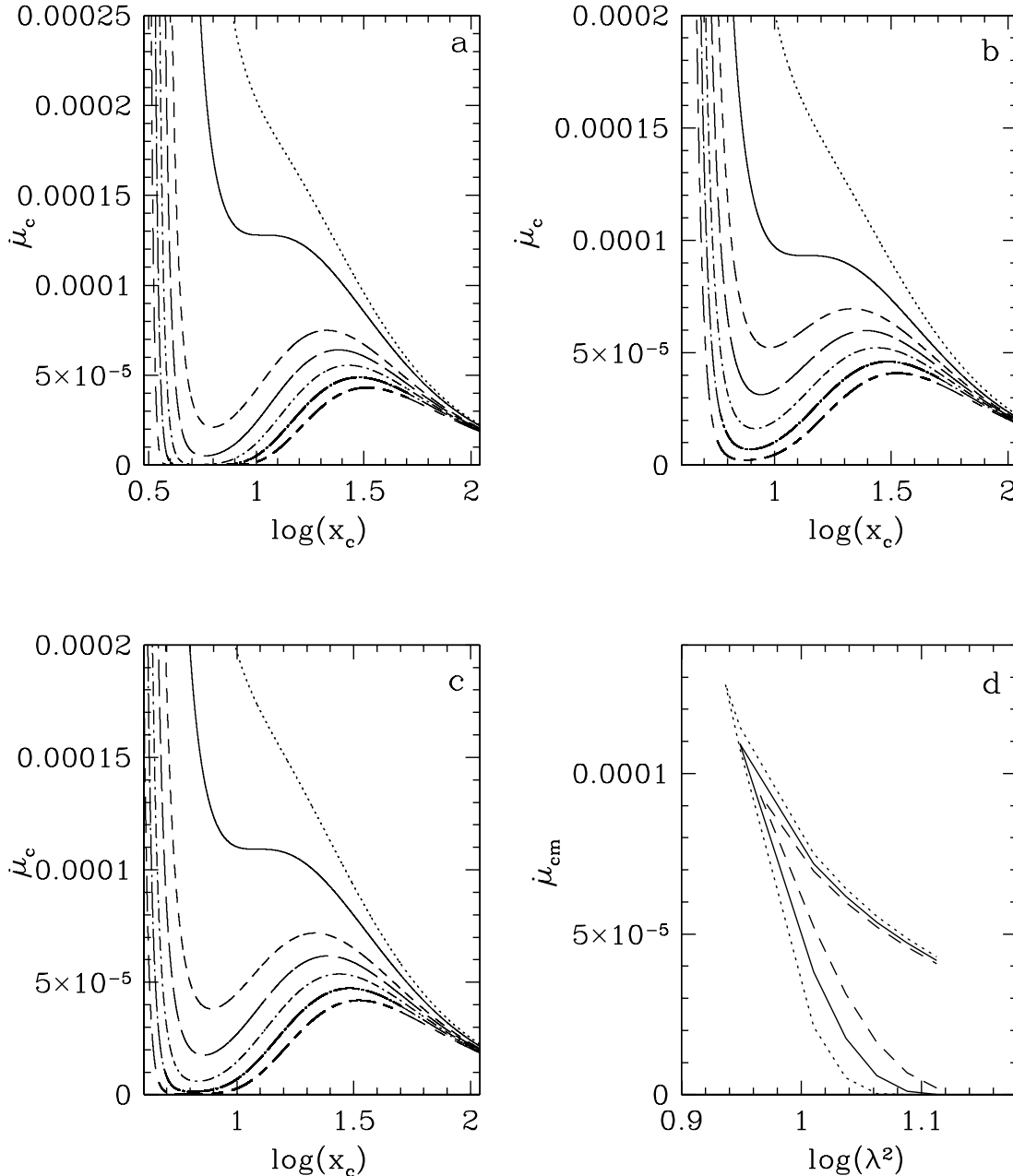


FIG. 2.—(a–c) Variation of entropy as a function of sonic location for a set of disk angular momentum ( $\lambda$ ), when (a)  $a = 0.5$ , (b)  $a = -0.5$ , and (c)  $a = 0$ . Solid curve indicates the flow with critical angular momentum ( $\lambda_c$ ) for which the flow has just a single critical point which is (a)  $\lambda_c = 2.94$ , (b)  $\lambda_c = 3.04$ , and (c)  $\lambda_c = 2.982$ . From the top to bottom curve,  $\lambda = 2.8, \lambda_c, 3.2, 3.3, 3.4, 3.5, 3.6$ . Any flow of  $\lambda > \lambda_c$  has three and  $\lambda < \lambda_c$  has one critical point. (d) Variation of extremum values of entropy for curves (a), (b), and (c) as a function of  $\lambda^2$  for  $a = 0$  (solid curve),  $a = 0.5$  (dotted curve), and  $a = -0.5$  (dashed curve).  $\gamma = 4/3$  for all the curves.

sonic points exist. As the angular momentum of accreting matter decreases, the possibility of forming three sonic points decreases. This is very well understood physically; as the angular momentum of accreting matter decreases, the disk tends to a *Bondi-Flow like* structure, which has single saddle-type sonic point. The solid curves of all three figures indicate the locus of sonic entropy with a single extremum point. Only the flows of angular momentum greater than that of the solid curve have three sonic points, otherwise for a particular flow, we have only one sonic point. In Figure 2d, we show the projection of all the curves in Figure 2a, 2b, and 2c to the  $\mathcal{M}_{\text{cm}}-\lambda^2$  plane, where  $\mathcal{M}_{\text{cm}}$  indicates the extremum entropy at the sonic points. Figure 2d indicates the valid physical parameter region of the accretion disk that has three sonic points in the flow. It should be noted

that, for a particular Kerr parameter, the accreting flow can have three sonic locations for different pairs of  $(\lambda, \mathcal{M}_{\text{cm}})$ . However, for a particular  $\lambda$ , if  $\mathcal{M}_{\text{cm}}$  decreases, the stability of the sonic points as well as that of the disk diminishes too. Thus, in a section of the diagram for particular  $a$ , all points are not an equally probable set of physical parameters in the formation of three sonic points. It is clear that, as the corotation of black hole increases, the parameter region enlarges, so that three sonic points may exist. Therefore, the disk with three sonic points becomes more probable at high corotation. On the other hand, this region decreases for the counterrotating flow. Similar features are noticed from Figure 3, where the variation of sonic energies are depicted. In a similar manner, Figure 3d indicates that the parameter space with three sonic points enlarges if the corotation of

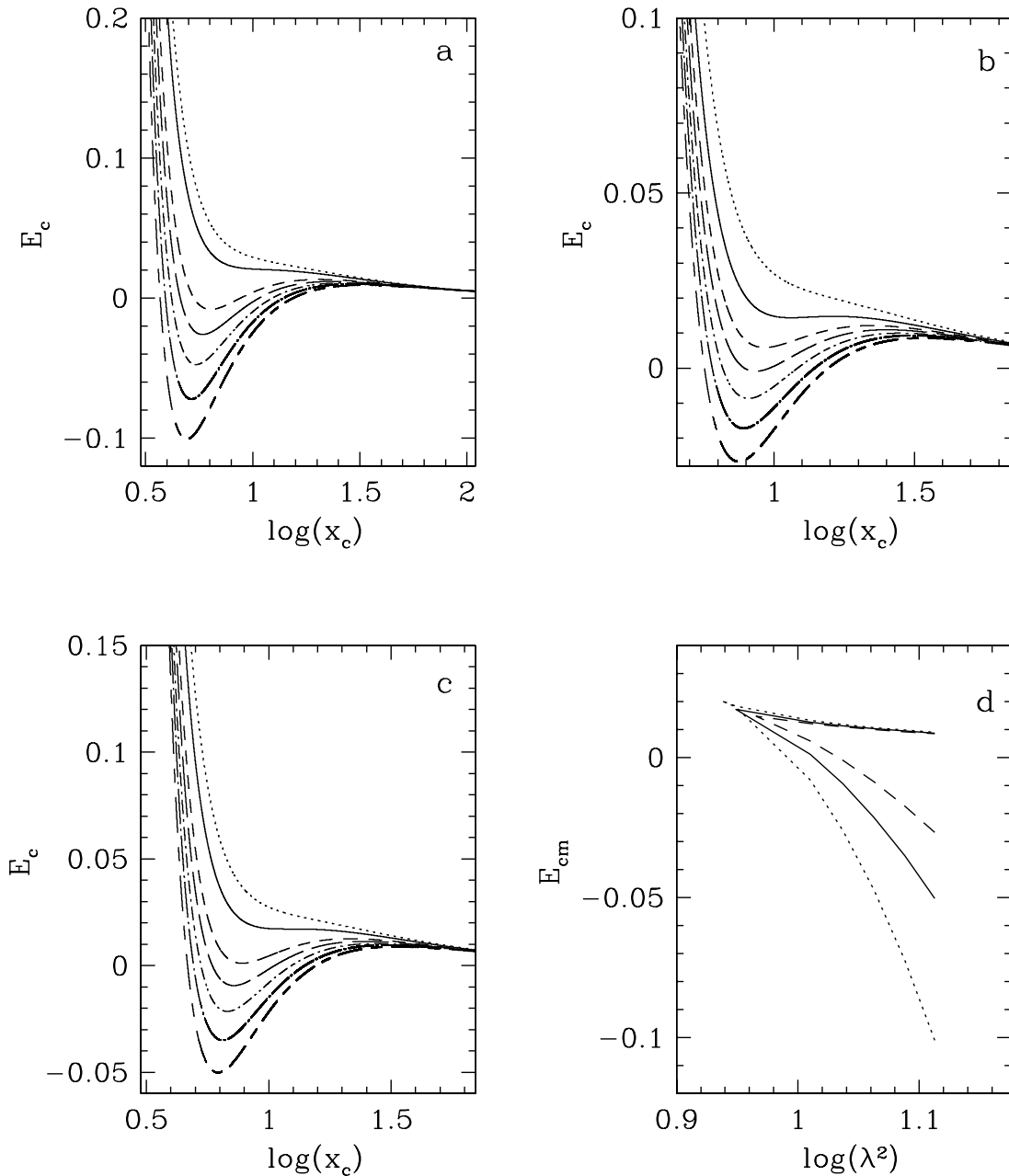


FIG. 3.—Same as Fig. 2 except the energy is plotted in place of entropy

the black hole increases, where  $E_{cm}$  indicates the extremum energy of the different curves in Figures 3a–3c. The physical reasons are the following. Higher corotation results in a shift of  $x_b$  and  $x_s$  to an edge of the accretion disk farther in and an enlargement of the stable disk region (as we know that the stable circular orbit is possible in the disk up to the radius  $x_s$ ). On the other hand, higher counterrotation results in an outward shift of  $x_b$  and  $x_s$ , and the size of the stable disk region decreases.

Figure 4 indicates the variation of energy with entropy at sonic locations for different Kerr parameters. “I” indicates the branch of inner “X-type” sonic point that is different for different Kerr parameters, while “O” indicates the outer

“X-type” sonic point branch. Along the O branch, all the curves (solid, dotted, and dashed) lie on top of each other. Therefore it is clear that the rotation of the black hole does not affect the outer “X-type” sonic point. Figures 4a and 4b show that with the increase of Kerr parameter (corotation), inner sonic points of the disk shift toward the lower-entropy region, and the disk becomes unstable. But the outer sonic point branch remains unchanged for all values of rotation. We know that, if there is a possibility of matter in the outer sonic point branch of lower entropy jumping to the inner sonic point branch of higher entropy, a shock can form in the accretion disk. As, with the increase of Kerr parameter, the inner sonic point branch shifts to the lower

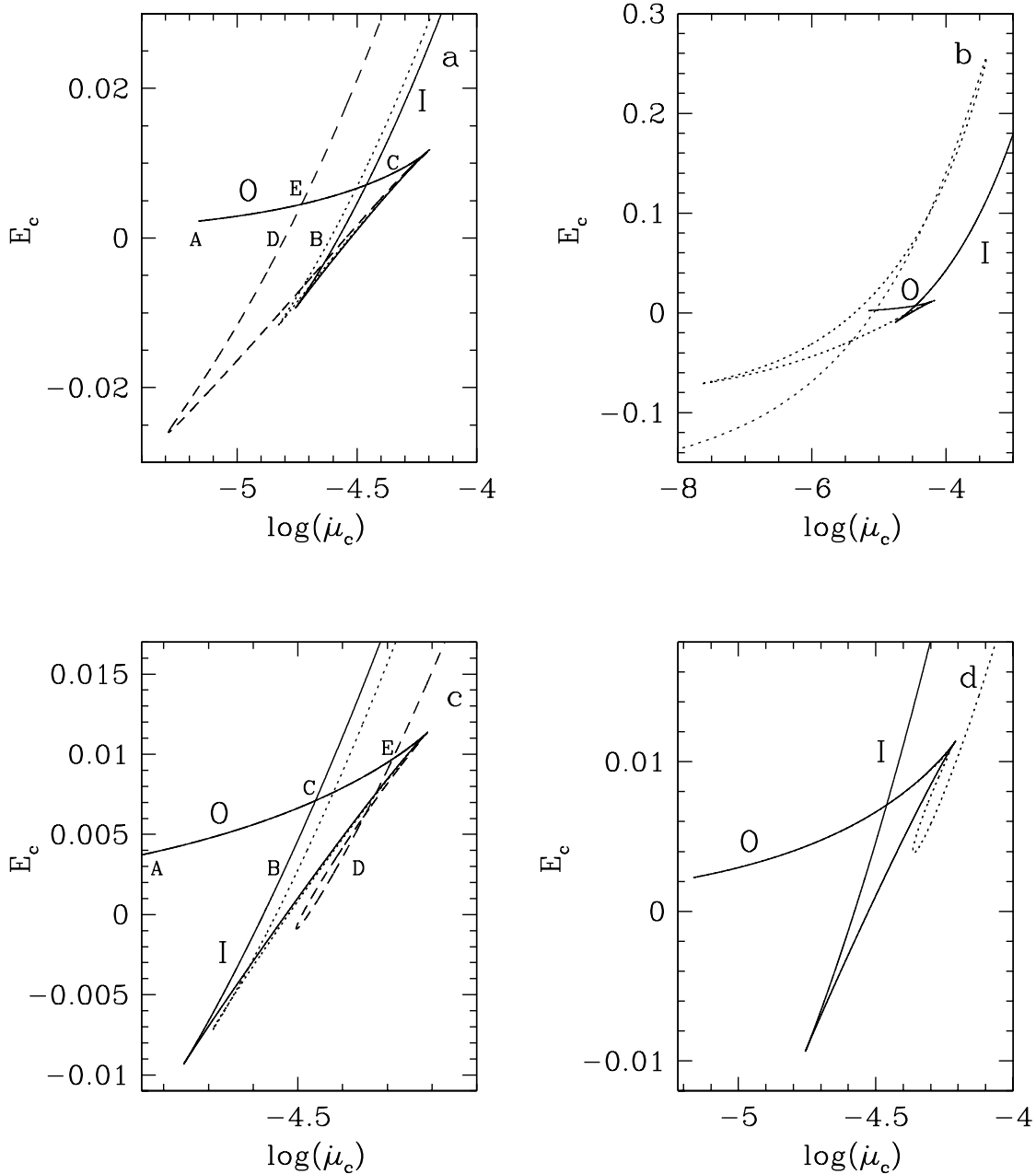


FIG. 4.—Variation of energy with entropy at sonic points when disk angular momentum  $\lambda = 3.3$  for (a)  $a = 0$  (solid curve),  $a = 0.1$  (dotted curve), and  $a = 0.5$  (dashed curve); (b)  $a = 0$  (solid curve) and  $a = 0.998$  (dotted curve); (c)  $a = 0$  (solid curve),  $a = -0.1$  (dotted curve), and  $a = -0.5$  (dashed curve); and (d)  $a = 0$  (solid curve) and  $a = -0.998$  (dotted curve). O and I indicate the branch of outer and inner sonic points, respectively, for  $a = 0$ .  $\gamma = 4/3$  for all the curves.

entropy region, the stability of both the shock and the disk is at stake. For example, in Figure 4a, if we join the points A, B and A, D, we will find two sections of the curve, namely, ABC (*solid curve*) and ADE (*dashed curve*) which are the parameter regions where the shock may form in the accretion disk for  $a = 0$  and  $a = 0.5$ , respectively. If we draw the lines of constant energy (which are horizontal in Fig. 4a), connecting the outer sonic point branch (AC for  $a = 0$  and AE for  $a = 0.5$ ), to the inner one (BC for  $a = 0$  and DE for  $a = 0.5$ ), section ABC will contain more lines with respect to section ADE (as the section ABC is bigger than ADE). On the other hand, a constant energy line indicates the possibility of a shock (as it shows the possibility of an increment of entropy in the flow, keeping the energy constant). Clearly, for a corotating black hole, the possibility of formation of a shock decreases, as well as the shock itself becomes unstable. The physical reason is that, with the increase of Kerr parameter, the angular momentum of the system increases, which helps the disk to maintain a high azimuthal speed of matter up to a very close proximity to the black hole, and as a result the radial matter speed can overcome the corresponding sound speed at an inner radius only. On the other hand, the inner edge of the accretion disk is comparatively less stable as the entropy decreases at lower radii. As the inner sonic points form at an inner radii, with the increase of  $a$ , the disk tends to an unstable situation that decreases the value of the entropy. Figure 4b shows that the possibility of a shock disappears completely when  $a = 0.998$ , as there is no transition possible from the outer to inner sonic branch that can increase the entropy of the system. Here, the inner edge is extremely unstable in such a manner that its entropy is even lower than that of the outer sonic point branch. As the inner edge of the disk spreads out for  $a = 0.998$ , there are two branches of the center-type sonic point.

In Figure 4c, the situation is opposite. As the counterrotation of the black hole increases in magnitude, the inner sonic point branch shifts toward a higher-entropy region. Thus, the disk, as well as the shock, becomes more stable. Still, the outer sonic point branch is not affected due to the rotation of black hole and the branches for different Kerr parameters are superimposed. In Figure 4c, the sections ABC (*solid curve*) and ADE (*dashed curve*) for  $a = 0$  and  $a = -0.5$ , respectively, show the regions where the shock may form in the disk. The physical reason to have a more stable inner sonic point branch for the counterrotating case is as follows. A higher counterrotation implies that the net angular momentum of the system decreases; as a result, the matter falls faster at larger radii, and it becomes supersonic at a comparatively outer edge of the disk that is more stable. In a similar manner, as explained for Figure 4a, the greater size of the section ADE than that of ABC implies a greater possibility of a shock. However, for a very high counterrotation of the black hole (see Fig. 4d), the entire system shifts to the outer side that is more stable, and the inner sonic point branch itself tends to merge with the branch of the outer sonic point. Since the net angular momentum of the system becomes very small for higher counterrotation, the corresponding centrifugal pressure onto the matter becomes insignificant; as a result, the possibility of shock formation diminishes again. Therefore, we can conclude that, if the angular momentum of the black hole increases or decreases significantly, the shock wave in the accretion disk becomes unstable and the disk itself loses stability.

#### 4. FLUID PROPERTIES OF ACCRETION DISK

We will discuss now the effect of rotation of the black hole on the disk fluid. In the previous section, we have already confirmed that the rotation significantly affects the global parameter space of the accretion disk. Our intention is to incorporate the rotation of the black hole and to see the change of fluid properties known for the nonrotating case.

Figure 5a shows the variation in Mach number for a particular set of physical parameters. If the black hole is chosen to be nonrotating, a shock forms in the disk. When rotation is considered, keeping other parameters unchanged, the solution changes and the shock disappears. If the black hole corotates, the inner edge of the disk becomes unstable, and the matter does not find any physical path to fall steadily into the black hole. On the other hand, if the black hole counterrotates, there is a single sonic point in the disk, and the matter attains supersonic speed only close to the black hole and falls into it. Thus, for the nonrotating and counterrotating cases, there are smooth solutions of matter passing through the inner sonic point, while for the corotating cases, it is not so. The physical reasons behind these phenomena can be explained as follows. When the black hole corotates, the angular momentum of the system increases, and the radial speed of the matter may not be able to overcome the centrifugal barrier to fall into the black hole for that parameter set. If the black hole counterrotates, the angular momentum of the system decreases, the centrifugal barrier smears out, and matter falls steadily into the black hole. It can be mentioned here that, for the other choice of physical parameters (e.g., reducing/increasing the angular momentum of accreting matter for co/counterrotation, changing the sonic locations, etc.), the shock may appear again, even for the rotating black holes (a few such examples are depicted in Fig. 6). Figure 5b shows the corresponding density profiles in units of  $c^6/G^3M^2$  for a particular accretion rate. As the matter slows down abruptly, the density of the disk fluid jumps up at the shock location for a nonrotating case. For the counterrotating black holes, the angular momentum of the system is less; thus, to overcome the centrifugal barrier, matter does not need to attain a high radial speed away from the black hole. In this situation, the radial matter speed is less and the corresponding density of accreting fluid is high compared to the nonrotating case. We also show the density profiles for corotating, unstable cases. In Figure 5c, we compare the corresponding temperature profiles in units of  $10^9$  K ( $T_9$ ). The variation of temperature is similar to that of density away from the black hole but is opposite when close to the horizon (as the density varies inversely with the temperature at a small  $x$  but not so at a large  $x$ ; see eq. [1]). As the higher counterrotation Mach number decreases, the temperature of the accretion disk becomes higher.

The variation of the shock invariant quantity,  $C$ , is shown in Figure 5d for the nonrotating case. The intersections between the solution of the inner and outer sonic point branches indicate the shock locations. Since the inner shock location is unstable, the only shock forms at an outer radius,  $x = 37.77$ .

Figure 6 gives examples where the shock forms in an accretion disk around a rotating black hole. The variation of Mach numbers for different Kerr parameters are shown in Figure 6a. It reflects that, for a small rotation of the black hole ( $a = 0.1$ ), matter adjusts the sonic locations in such a

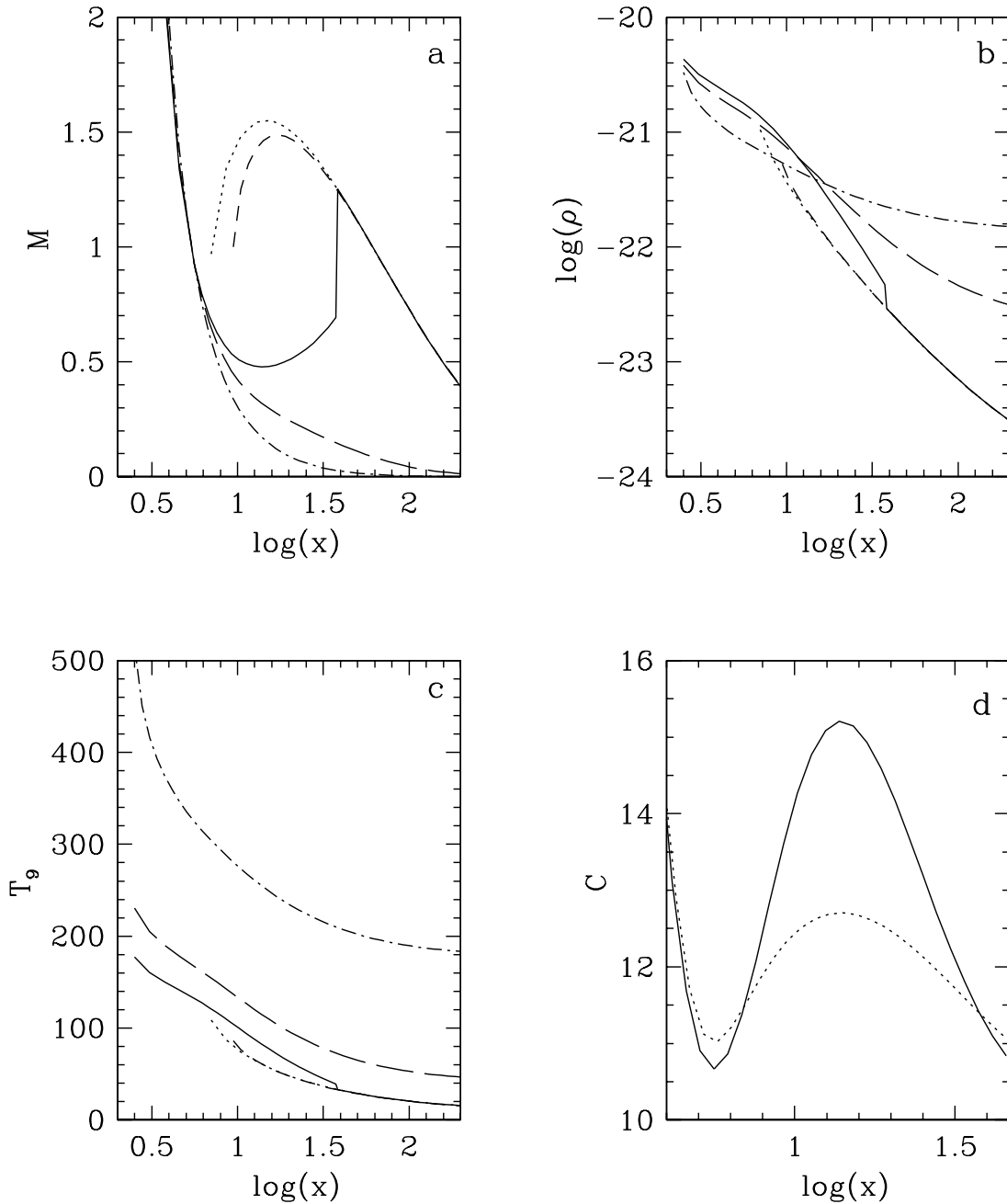


FIG. 5.—Variation of (a) Mach number, (b) density, and (c) temperature in units of  $10^9$  K as a function of radial coordinate for  $a = 0$  (solid curve),  $a = 0.1$  (dotted curve),  $a = 0.5$  (dashed curve),  $a = -0.1$  (long-dashed curve), and  $a = -0.5$  (dot-dashed curve). (d) Variation of shock invariant quantity ( $C$ ) as a function of radial coordinate for inner sonic (solid curve) and outer sonic (dotted curve) point branch when  $a = 0$ ; the intersection points of two curves indicate the shock locations, which are  $x_s = 33.77, 6.94$ . Other parameters are  $M = 10 M_\odot$ ,  $\dot{M} = 1$  Eddington rate,  $\lambda = 3.3$ ,  $x_o = 70$  (solid, dotted, and dashed curves),  $x_i = 5.6$  (solid, long-dashed, and dot-dashed curves),  $\gamma = 4/3$ .

manner that the outer ( $x_o$ ) and inner ( $x_i$ ) sonic locations shift to a more outer and more inner region, respectively, with respect to a nonrotating case, and the shock forms in the disk at  $x = 17.18$ . For the counterrotating case ( $a = -0.1$ ),  $x_o$  may remain unchanged, but  $x_i$  has to be shifted outside to form a shock at  $x = 17.25$  (that keeps the shock location [almost] unchanged). As for the counterrotating cases, marginally stable ( $x_s$ ) and marginally bound ( $x_b$ ) orbits shift away from the black hole with respect to a corotating one;  $x_i$  also shifts outside to stabilize the disk. If the corotation of the black hole is higher, say  $a = 0.5$ , to

form a stable shock, not only the inner sonic location has to be smaller, but the disk angular momentum ( $\lambda$ ) should also be reduced. High rotation of a black hole results in the location of horizon ( $x_+$ ) as well as  $x_b$  and  $x_s$  shifting inward, and the matter attains a supersonic speed at a point further inside of the inner edge of the disk to fall into the black hole. Thus all the phenomena, e.g., sonic transitions, shock formations, etc., shift inside. Moreover, for the stable solution, the angular momentum of the system cannot be very high, otherwise matter will be unable to overcome the centrifugal barrier. Thus, for the high rotation of a black hole, like

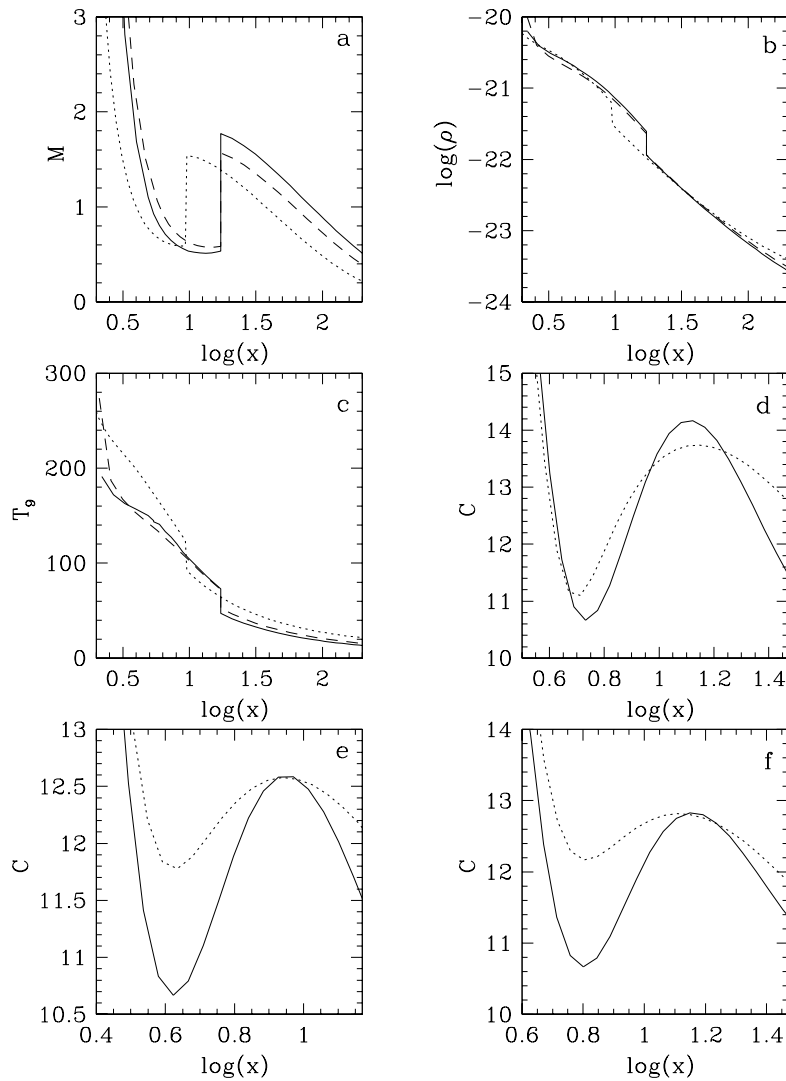


FIG. 6.—Variation of (a) Mach number, (b) density, and (c) temperature in unit of  $10^9$  K as a function of radial coordinate when the sets of physical parameters are (i)  $a = 0.1$ ,  $x_o = 94$ ,  $x_i = 5.4$ ,  $\lambda = 3.3$  (solid curve); (ii)  $a = 0.5$ ,  $x_o = 43$ ,  $x_i = 4.2$ ,  $\lambda = 2.8$  (dotted curve), and (iii)  $a = -0.1$ ,  $x_o = 70$ ,  $x_i = 6.324$ ,  $\lambda = 3.3$  (dashed curve). Variation of shock invariant quantity,  $C$ , as a function of radial coordinate for the set of (d) parameter (i) when  $x_s = 17.18, 9.2$ ; (e) parameter (ii) when  $x_s = 9.51, 8.35$ ; and (f) parameter (iii) when  $x_s = 17.25, 13.73$ . Solid and dotted curves are for inner and outer sonic branches, respectively. Other parameters are  $M = 10 M_\odot$ ,  $\dot{M} = 1$  Eddington rate, and  $\gamma = 4/3$ .

$a = 0.5$ ,  $\lambda$  has to be reduced to form a shock (at  $x = 9.51$ ) and stabilize the disk. However, for  $a = -0.5$  and less, there is no sub-Keplerian flow for which a shock may form. For the higher counterrotation of a black hole, the angular momentum of the system decreases. Since a higher centrifugal barrier is essential to form a shock, at the higher counterrotation, the shock completely disappears from the accretion disk. Figures 6b and 6c show the corresponding variations of density and temperature, respectively. In Figures 6d, 6e, and 6f, we show the corresponding variation of shock invariant quantity  $C$  for the inner and outer sonic point branches, when  $a = 0.1, 0.5, -0.1$ , respectively. Again it becomes clear that, for the faster rotation of a black hole, the shock location shifts inside the disk.

In Figure 7, we show the fluid properties for  $a = \pm 0.998$ . At a very high rotation of black hole, the possibility to form a shock in the accretion disk totally disappears. For the corotating case, the disk cannot be stable unless the angular momentum of accreting matter is very low (as we have already mentioned that the high angular momentum of the

system makes the disk unstable). Therefore, there is no scope to form a shock, as to its formation, matter needs a significant centrifugal barrier as well as a high angular momentum of the accreting fluid. Here we choose  $\lambda = 1.8$ , and the matter falls almost freely. For the counterrotating case, the matter angular momentum need not be low to stabilize the disk. However, in the sub-Keplerian accretion disk,  $\lambda$  cannot attain a high value to increase the angular momentum as well as the centrifugal barrier of a system to form a shock. Thus, the shock also disappears for a high counterrotating case. Figure 7a shows that  $x_b$  and  $x_s$  shift outward for the retrograde orbit, and the matter attains a supersonic speed at a radius farther out than in the case of a direct orbit of the disk. However, far away from black hole, the radial velocity is less (as it needs to overcome a smaller centrifugal barrier) than that of the corotating case. Figure 7b shows the variation of corresponding density. Lower velocity implies a high rate of piling up of matter at a particular radius that produces a high density in the disk and thus, the density behaves in an opposite manner to Mach number.

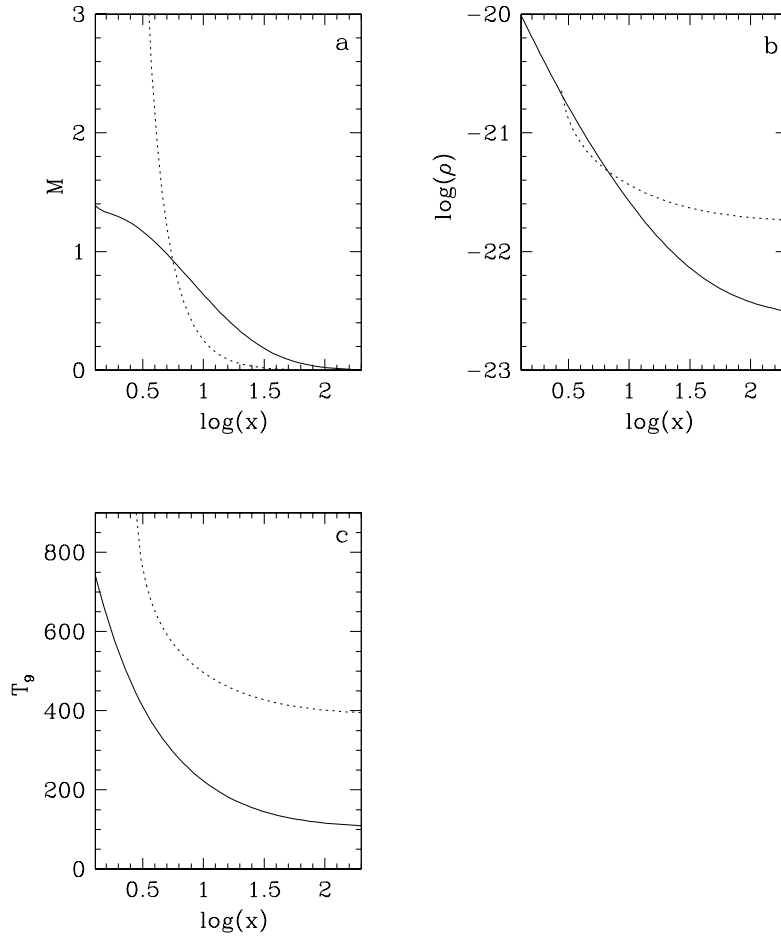


FIG. 7.—Variation of (a) Mach number, (b) density, and (c) temperature in units of  $10^9$  K as a function of radial coordinate for the sets of parameters (i)  $a = 0.998$ ,  $x_i = 5.6$ ,  $\lambda = 1.8$  (solid curve) and (ii)  $a = -0.998$ ,  $x_i = 5.6$ ,  $\lambda = 3.3$  (dotted curve). Other parameters are  $M = 10 M_\odot$ ,  $\dot{M} = 1$  Eddington rate, and  $\gamma = 4/3$ .

Figure 7c shows the variation of virial temperature in the accretion disk. The temperature is low for corotation and high for counterrotation. The physical reason behind it is as follows. For corotation, the net speed as well as the kinetic energy of matter is lower, producing a lower temperature. On the other hand, for a counterrotating case, the situation is opposite. Although we show the virial temperature of the disk, in reality several cooling processes may take place that can reduce the disk temperature by up to 2 orders of magnitude.

## 5. DISCUSSION AND CONCLUSION

Here we have studied the stability of accretion disks around rotating black holes in a pseudo-Newtonian approach. Following Paper I, we have incorporated the general relativistic effects (according to Kerr geometry) on the accretion disk in such a manner that all the essential relativistic properties, e.g., the locations of the marginally bound and stable orbits, black hole horizon and mechanical energy of the accreting matter are reproduced in the disk for various values of Kerr parameters. Thus we can say our method is “pseudo-general-relativistic.” As our interest is to check how the rotation of a black hole solely affects the disk structure, we have chosen inviscid fluid in the accretion disk. Most of the earlier studies on structure and stability analysis

of the accretion disk have been done around a nonrotating black hole (Schwarzschild geometry). As no cosmic object is static, it is very important to consider the effect of rotation of the black hole, particularly for the discussion of an inner edge of an accretion disk. We have found that when the rotation of a black hole is incorporated, the valid, known disk parameter region of a nonrotating black hole is dramatically affected. As a result, the location of various sonic points and the shock (if any) get shifted severely and influence the disk structure. Therefore, we can conclude that in the study of an accretion disk, the rotation should be considered. Any related conclusion depends on the rotation parameter of a black hole. So, we can say that the known physical parameter regime (Chakrabarti 1989, 1990, 1996a) to form a shock, sonic locations, etc., in the disk around a nonrotating black hole is not global. The mentioned disk properties and phenomena not only get modified and/or shifted in location at the disk but also sometimes completely disappear. In our study, we have chosen the Kerr parameter from  $a = 0$  to the case of an extremely high rotation as  $a = 0.998$ , and thus, we now have a clear global picture of the accretion disk.

Although, in the literature, there are a few works on the accretion disk around Kerr black holes (e.g. Chakrabarti 1996b, 1996c; Gammie & Popham 1998; Popham & Gammie 1998), those do not concentrate on the comparative

study of a rotating and nonrotating black hole and the instability of disk induced by the rotation of black hole. Chakrabarti (1996b, 1996c) mainly concentrated on fast-rotating black holes and showed solution topology in full Kerr geometry. He does not show how the solution varies with the change of rotation of the black hole, keeping unchanged other physical parameters. Thus, it is not clear from those works how the Kerr parameter affects the disk solution solely. On the other hand, Gammie & Popham (1998) and Popham & Gammie (1998) do not discuss the effect of rotation on the sonic points globally, which is shown here in Figures 1–4. However, the fluid dynamical results achieved by them agree with the present work. For example, they (Gammie & Popham 1998; Popham & Gammie 1998) showed that the effect of nonzero Kerr parameter is dominant close to the black hole. That is also reflected in Figure 4 of the present work, which shows that the outer sonic point branches are unchanged, while the inner ones are shifted. They also showed that the (inner) sonic points move to smaller (larger) radii as corotation (counterrotation) increases in magnitude. In our work, similar features come out from Figures 1, 2, 3, and 6. Thus, we can conclude once again that the pseudopotential prescribed in Paper I can reproduce the general relativistic properties in accretion disk. Unlike the works by Gammie & Popham (1998) and Popham & Gammie (1998), here we have chosen inviscid flow to understand the sole effect of rotation of the black hole on the fluid and corresponding disk structure. Finally, we can conclude that the effect is significant.

Here we have carried out the stability analysis of the accretion disk by choosing the black hole to be rotating. Prasanna & Mukhopadhyay (2003) have worked on the stability of accretion disks around rotating compact objects (but not for black holes) in a perturbative approach. They incorporated the rotational effect of central object in a disk indirectly, by the inclusion of Coriolis acceleration term. Here, the compact object is a black hole and its rotational effect is brought from the Kerr metric only. As we have a very self-consistent pseudopotential (Paper I), it has been easy to study the accretion phenomena around a rotating black hole.

From the global analysis of sonic points, we have established that the disk becomes unstable for a higher corotation at a particular angular momentum of the accreting matter. On the other hand, to form a shock, the accretion disk must have a stable inner sonic point. Thus, for higher  $a$  (Kerr parameter), the shock is unstable, as the inner region of disk itself is not stable. In that regime, the shock may disappear by any disturbance created on the accreting matter, and thus the matter may not get a steady inner sonic point to form a stable inner disk. For the counterrotating cases, the angular momentum of the system decreases, and the matter falls to the black hole more rapidly. As there is no significant centrifugal barrier to slow down the matter, the possibility of shock decreases again. For a very high counterrotation,

shock disappears completely. Thus we can conclude that the parameter region where the shock is expected to form (Chakrabarti 1989, 1990, 1996a) for nonrotating black holes gets affected for the rotating ones. For a positive  $a$ , the shock might have been formed for a lesser value of the angular momentum of accreting matter. On the other hand, for a negative  $a$ , to form a shock, the angular momentum of accreting matter should have a larger value than that of nonrotating cases. As we are studying the sub-Keplerian accretion flow, the angular momentum of matter cannot be unlimitedly high (e.g., for a nonrotating black hole,  $\lambda \lesssim 3.6742$  at last stable orbit). Thus, to form a shock, matter cannot attain the angular momentum beyond a certain limit. Also for a highly corotating black hole, to stabilize the disk,  $\lambda$  has to be reduced by some physical process, otherwise the radial speed could not overcome the centrifugal pressure to form a steady inner edge of the disk. Therefore, the disk would not be transonic and could be unstable in this situation. Because of a reduced  $\lambda$ , centrifugal force as well as shock strength decreases; as a result, the possibility of a shock is also reduced for both the corotating and counterrotating black holes. However, at an intermediate corotation, the parameter region of the accretion disk enlarges, having three sonic points, and there is a possibility of a stable shock formation. On the other hand, for a counterrotation, the valid parameter region with three sonic points at the disk shortens, and thus, the possibility of shock reduces.

Now the question may arise, how would a flow behave in the region where sonic points disappear because of the higher rotation of black hole? It may be that matter would try to pass through same sonic point as of nonrotating (or slowly rotating) case. Because of the absence of sonic points, the searching procedure for the true sonic location should give rise to an unstable solution. Only the time-dependent simulation of accretion disk can tell whether this idea is correct or not. Overall we can say that the rotation of a black hole affects the sonic locations of an accretion disk that are directly related to the formation of stable disk structure. Therefore, the stability of an accretion disk is strongly related to the rotation of the central black hole.

It has also been confirmed that the potential given in Paper I is very well applicable for the global solution and corresponding fluid dynamical study of the accretion disk around a rotating black hole. The set of full general relativistic disk equations is very complicated for a Kerr black hole, particularly when the accreting fluid is chosen to be viscous. Thus, in the study of a relativistic accretion disk, this pseudopotential is very effective to avoid the complexities of full general relativistic fluid equations. The next step should be the study of a viscous accretion disk using this general pseudopotential.

I am grateful to my friend Subharthi Ray (of IF-UFF) for carefully reading the manuscript and amending the grammatical errors.

#### REFERENCES

- Abramowicz, M., Chen, X.-M., Granath, M., & Lasota, J.-P. 1996, *ApJ*, 471, 762  
 Abramowicz, M., Czerny, B., Lasota, J., & Szuszkiewicz, E. 1988, *ApJ*, 332, 646  
 Abramowicz, M., & Kato, S. 1989, *ApJ*, 336, 304  
 Abramowicz, M., & Zurek, W. 1981, *ApJ*, 246, 314  
 Chakrabarti, S. K. 1989, *ApJ*, 347, 365  
 ———. 1990, *Theory of Transonic Astrophysical Flows* (Tasker Town: World Scientific)  
 Chakrabarti, S. K. 1996a, *ApJ*, 464, 664  
 ———. 1996b, *MNRAS*, 283, 325  
 ———. 1996c, *ApJ*, 471, 237  
 Gammie, C., & Popham, R. 1998, *ApJ*, 498, 313  
 Kato, S., Fukue, J., & Mineshige, S. 1998, *Black Hole Accretion Discs* (Kyoto: Kyoto Univ. Press)  
 Landau, L. D., & Lifshitz, E. M. 1987, *Fluid Mechanics* (Burlington: Butterworth-Heinemann)  
 Lu, J.-F., & Yuan, F. 1998, *MNRAS*, 295, L66

- Manmoto, T. 2000, ApJ, 534, 734  
Matsumoto, R., Kato, S., Fukue, J., & Okazaki, A. T. 1984, PASJ, 36, 71  
Miwa, T., Fukue, J., Watanabe, Y., & Katayama, M. 1998, PASJ, 50, 325  
Mukhopadhyay, B. 2002a, Int. J. Mod. Phys. D, 11, 1305  
———. 2002b, ApJ, 581, 427 (Paper I)  
Mukhopadhyay, B., & Chakrabarti, S. K. 2001, ApJ, 555, 816  
Narayan, R., Barret, D., & McClintock, J. 1997, ApJ, 482, 448  
Narayan, R., Mahadevan, R., Grindlay, J., Popham, R., & Gammie, C. 1998, ApJ, 492, 554  
Narayan, R., & Yi, I. 1994, ApJ, 428, L13  
Novikov, I. D., & Thorne, K. S. 1973, in Black Holes, Les Houches 1972 (France), ed. B. Dewitt & C. DeWitt (New York: Gordon & Breach), 343  
Paczynski, B., & Wiita, P. 1980, A&A, 88, 23  
Page, D., & Thorne, K. S. 1974, ApJ, 191, 499  
Peitz, J., & Appl. S. 1997, MNRAS, 286, 681  
Popham, R., & Gammie, C. 1998, ApJ, 504, 419  
Prasanna, A. R., & Mukhopadhyay, B. 2003, Int. J. Mod. Phys. D, 12, 157  
Shakura, N. I., & Sunyaev, R. A. 1973, A&A, 24, 337  
Sponholz, H., & Molteni, D. 1994, MNRAS, 271, 233